

Supporting Information

Isolated Mixed-Valence Iron Vanadium Malate and Its Metal Hydrates ($M = Fe^{2+}, Cu^{2+}, Zn^{2+}$) with Reversible and Irreversible Adsorptions for Oxygen

Wan-Ting Jin,^a Chang Yuan,^a Lan Deng,^a Dong-Li An,^a and Zhao-Hui Zhou^{*a}

^a State Key Laboratory of Physical Chemistry of Solid Surfaces, College of Chemistry and Chemical Engineering, Xiamen University, Xiamen, 361005, People's Republic of China. E-mail for Zhao-Hui Zhou: zhzhou@xmu.edu.cn.

Figure S1. Packing diagrams of crystal structures in 1 ~ 4 underlining the organizations of the $[Fe_2V_6O_{11}(mal)_6]^{6-}$ clusters by octahedral coordinated $[M(H_2O)_2]^{2+}$ ($M = Fe, Cu, Zn$), with an interlayer spacing of 3.56, 3.03, 2.84 and 3.00 Å respectively.	3
Figure S2. XPS spectrum of $(NH_4)_{3n}[Fe(H_2O)_2]_{1.5n}[Fe_2V_6O_{11}(mal)_6]_n \cdot 7.5nH_2O$ (2-Fe).	4
Figure S3. TG curves of solid $(NH_4)_3(NH_3CH_3)_3[Fe_2V_6O_{11}(mal)_6] \cdot 7.5H_2O$ (1).	5
Figure S4. TG curves of solid $(NH_4)_{3n}[Fe(H_2O)_2]_{1.5n}[Fe_2V_6O_{11}(mal)_6]_n \cdot 7.5nH_2O$. (2-Fe).	6
Figure S5. TG curves of solid $K_{3n}[Cu(H_2O)_2]_{1.5n}[Fe_2V_6O_{11}(mal)_6]_n \cdot 10nH_2O$ (3-Cu).	7
Figure S6. TG curves of solid $K_{3n}[Zn(H_2O)_2]_{1.5n}[Fe_2V_6O_{11}(mal)_6]_n \cdot 6.5nH_2O$ (4-Zn).	8
Figure S7. The experimental and simulated PXRD patterns of 2-Fe	9
Figure S8. The experimental and simulated PXRD patterns of 3-Cu	10
Figure S9. The experimental and simulated PXRD patterns of 4-Zn	11
Figure S10. N_2 adsorption-desorption isotherms of 2 ~ 4 at 77K.	12
Figure S11. Linear fits of O_2 adsorptions and desorptions at 298 K for 2 ~ 4	13
Figure S12. Linear fits of O_2 adsorptions at 308 K for 2 ~ 4	14
Figure S13. Isosteric heat of adsorption (Q_{st}) plotted against O_2 uptake for 2 ~ 4	15
Figure S14. FT-infrared spectra of $(NH_4)_3(NH_3CH_3)_3[Fe_2V_6O_{11}(mal)_6] \cdot 7.5H_2O$ (1), $(NH_4)_{3n}[Fe(H_2O)_2]_{1.5n}[Fe_2V_6O_{11}(mal)_6]_n \cdot 7.5nH_2O$ (2-Fe), $K_{3n}[Cu(H_2O)_2]_{1.5n}[Fe_2V_6O_{11}(mal)_6]_n \cdot 10nH_2O$ (3-Cu) and $K_{3n}[Zn(H_2O)_2]_{1.5n}[Fe_2V_6O_{11}(mal)_6]_n \cdot 6.5nH_2O$ (4-Zn).	16
Figure S15. FT-infrared spectra of 2-Fe , 2-Fe-O₂ . The sample of 2-Fe-O₂ were treated with O_2 adsorption.	17
Figure S16. Diffused reflectance spectra of solids $(NH_4)_3(NH_3CH_3)_3[Fe_2V_6O_{11}(mal)_6] \cdot 7.5H_2O$ (1), $(NH_4)_{3n}[Fe(H_2O)_2]_{1.5n}[Fe_2V_6O_{11}(mal)_6]_n \cdot 7.5nH_2O$ (2-Fe), $K_{3n}[Cu(H_2O)_2]_{1.5n}[Fe_2V_6O_{11}(mal)_6]_n \cdot 10nH_2O$ (3-Cu) and $K_{3n}[Zn(H_2O)_2]_{1.5n}[Fe_2V_6O_{11}(mal)_6]_n \cdot 6.5nH_2O$ (4-Zn).	18
Figure S17. The solid diffused spectra of 2-Fe and 2-Fe-O₂ . The sample of 2-Fe-O₂ were treated with O_2 adsorption.	19

Figure S18. The EPR spectra of 1 , 2-Fe and 4-Zn in solid state at 100 K	20
Table S1. Crystallographic data and structural refinement details for $(NH_4)_3(NH_3CH_3)_3[Fe_2V_6O_{11}(mal)_6] \cdot 7.5H_2O$ (1), $(NH_4)_3n[Fe(H_2O)_2]_{1.5n}[Fe_2V_6O_{11}(mal)_6]_n \cdot 7.5nH_2O$ (2-Fe), $K_{3n}[Cu(H_2O)_2]_{1.5n}[Fe_2V_6O_{11}(mal)_6]_n \cdot 10nH_2O$ (3-Cu) and $K_{3n}[Zn(H_2O)_2]_{1.5n}[Fe_2V_6O_{11}(mal)_6]_n \cdot 6.5nH_2O$ (4-Zn).	21
Table S2. Selected bond distances (Å) and angles (°) for $(NH_4)_3(NH_3CH_3)_3[Fe_2V_6O_{11}(mal)_6] \cdot 7.5H_2O$ (1).....	22
Table S3. Selected bond distances (Å) and angles (°) for $(NH_4)_3n[Fe(H_2O)_2]_{1.5n}[Fe_2V_6O_{11}(mal)_6]_n \cdot 7.5nH_2O$ (2-Fe).	24
Table S4. Selected bond distances (Å) and angles (°) for $K_{3n}[Cu(H_2O)_2]_{1.5n}[Fe_2V_6O_{11}(mal)_6]_n \cdot 10nH_2O$ (3-Cu).	25
Table S5. Selected bond distances (Å) and angles (°) for $K_{3n}[Zn(H_2O)_2]_{1.5n}[Fe_2V_6O_{11}(mal)_6]_n \cdot 6.5nH_2O$ (4-Zn).	26
Table S6. Comparisons of selected bond distances (Å) in 1 ~ 4	27
Table S7. Select bond distances (Å) and angles (°) of FeV-co ² and 2-Fe	28
Table S8. Bond valence calculations for end-capped iron and bridging metals in 1 ~ 4	29
Table S9. Bond valence calculations for vanadium centers in 1 ~ 4	30
Table S10. Adsorption data of O ₂ , CO ₂ , CH ₄ , N ₂ and H ₂ (mg/g) of 3-Cu at 298 K under different pressures respectively.	31
Table S11. Adsorption and desorption data of O ₂ (mg/g) of 2-Fe , 3-Cu , 4-Zn at 298 K under different pressures respectively.....	32
Table S12. Adsorption data of O ₂ (mg/g) of 2-Fe , 3-Cu , 4-Zn at 308 K under different pressures respectively.	33
References	34

Figure S1. Packing diagrams of crystal structures in **1** ~ **4** underlining the organizations of the $[\text{Fe}_2\text{V}_6\text{O}_{11}(\text{mal})_6]^{6-}$ clusters by octahedral coordinated $[\text{M}(\text{H}_2\text{O})_2]^{2+}$ ($\text{M} = \text{Fe}, \text{Cu}, \text{Zn}$), with an interlayer spacing of 3.56, 3.03, 2.84 and 3.00 Å respectively.

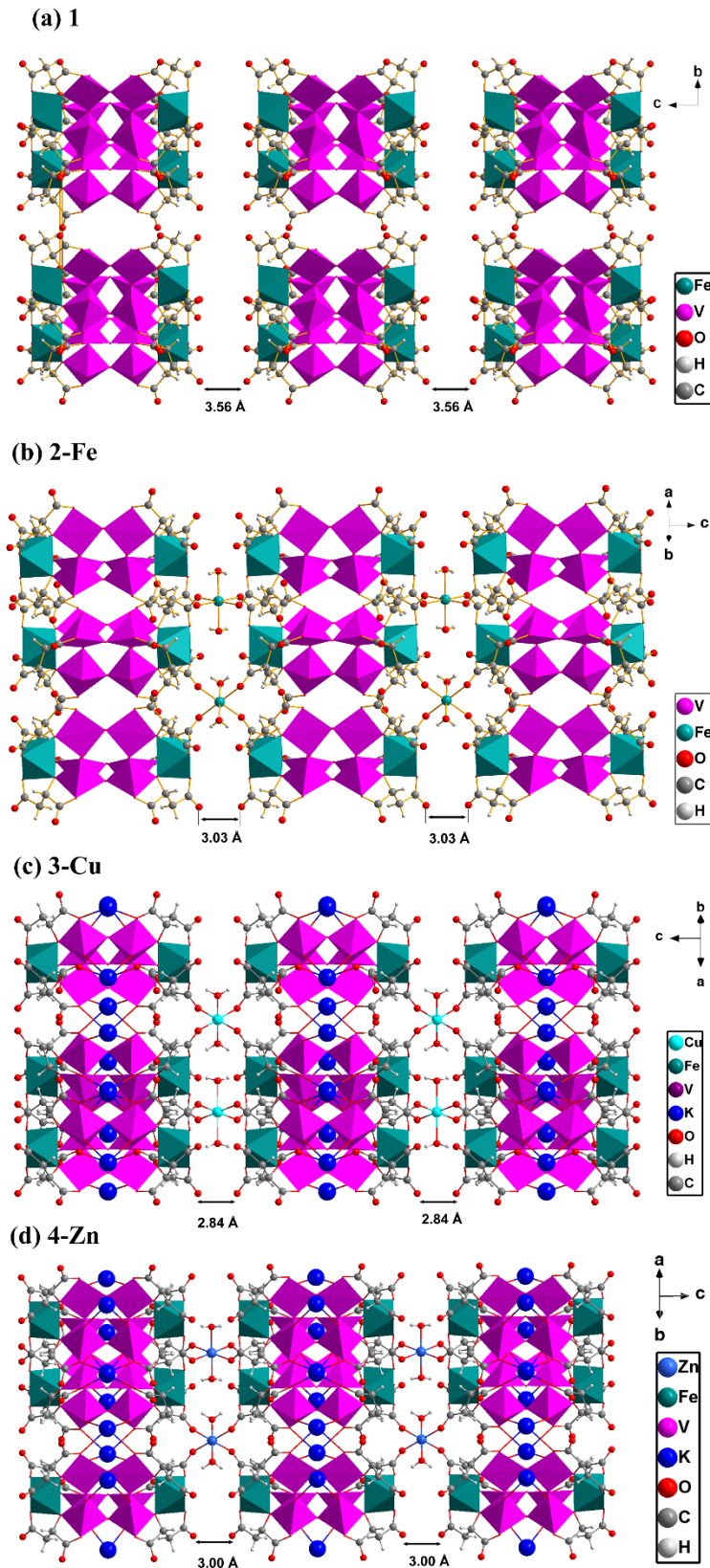
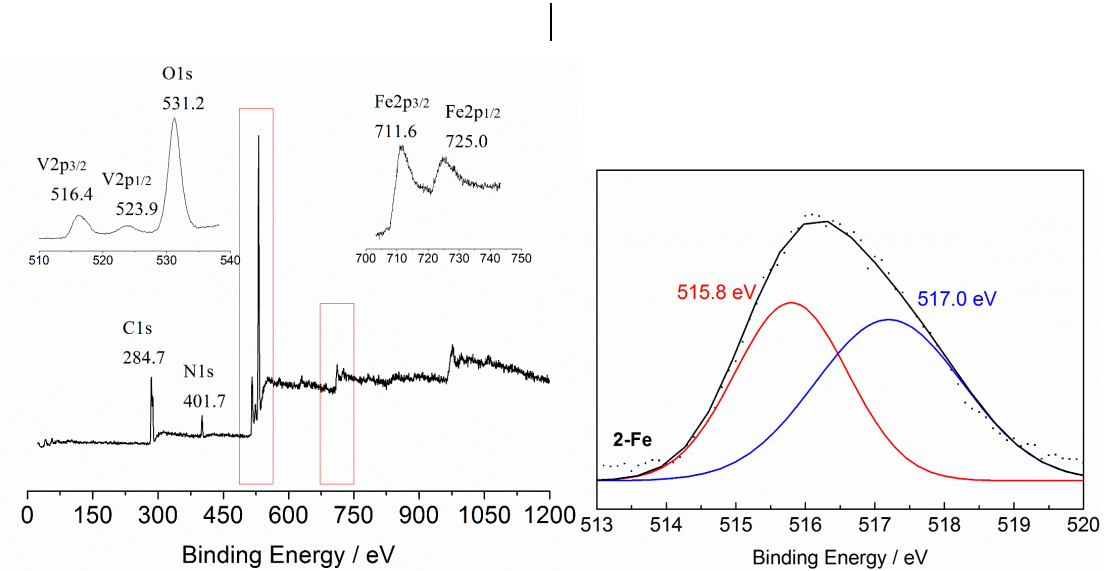


Figure S2. XPS spectrum of $(\text{NH}_4)_3\text{n}[\text{Fe}(\text{H}_2\text{O})_2]_{1.5\text{n}}[\text{Fe}_2\text{V}_6\text{O}_{11}(\text{mal})_6]_{\text{n}} \cdot 7.5\text{nH}_2\text{O}$ (**2-Fe**).



The distribution of the oxidation states in cluster **2-Fe** was measured by X-ray photoelectron spectroscopy (XPS). One broad peak at 516.4 eV was observed. The peak-differentiating analysis gives two peaks at 515.8 and 517.0 eV with a ratio of 1:2, attributed to V^{4+} 2p_{3/2} and V^{5+} 2p_{3/2}, respectively.¹ The formal oxidation state of $\text{V}^{\text{IV}}_2\text{V}^{\text{V}}_4$ from XPS is consistent with the charge balance observed from crystal structure.

Figure S3. TG curves of solid $(\text{NH}_4)_3(\text{NH}_3\text{CH}_3)_3[\text{Fe}_2\text{V}_6\text{O}_{11}(\text{mal})_6] \cdot 7.5\text{H}_2\text{O}$ (**1**).

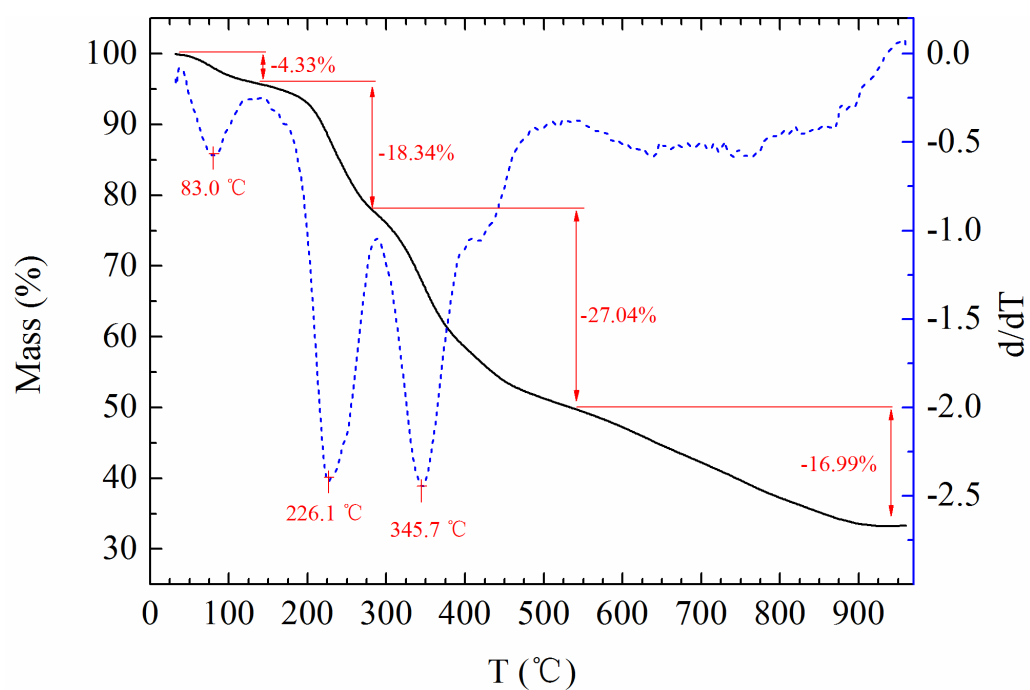


Figure S4. TG curves of solid $(\text{NH}_4)_{3n}[\text{Fe}(\text{H}_2\text{O})_2]_{1.5n}[\text{Fe}_2\text{V}_6\text{O}_{11}(\text{mal})_6]_n \cdot 7.5n\text{H}_2\text{O}$. (2-Fe).

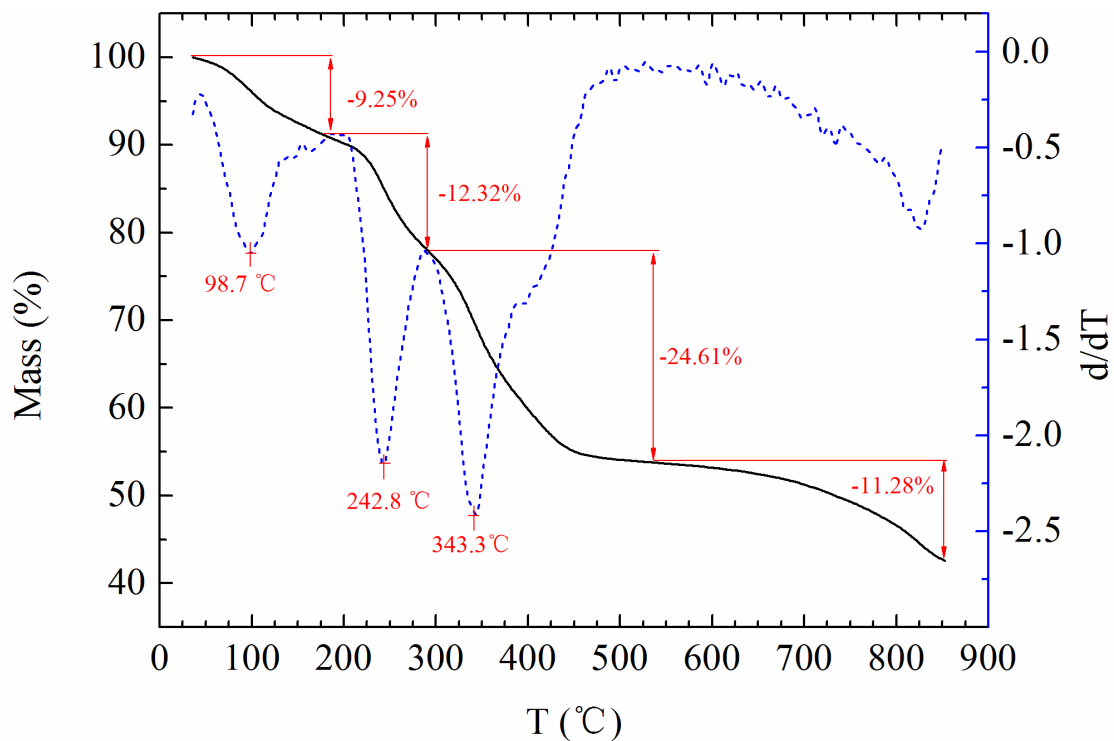


Figure S5. TG curves of solid $K_{3n}[Cu(H_2O)_2]_{1.5n}[Fe_2V_6O_{11}(mal)_6]_n \cdot 10nH_2O$ (**3-Cu**).

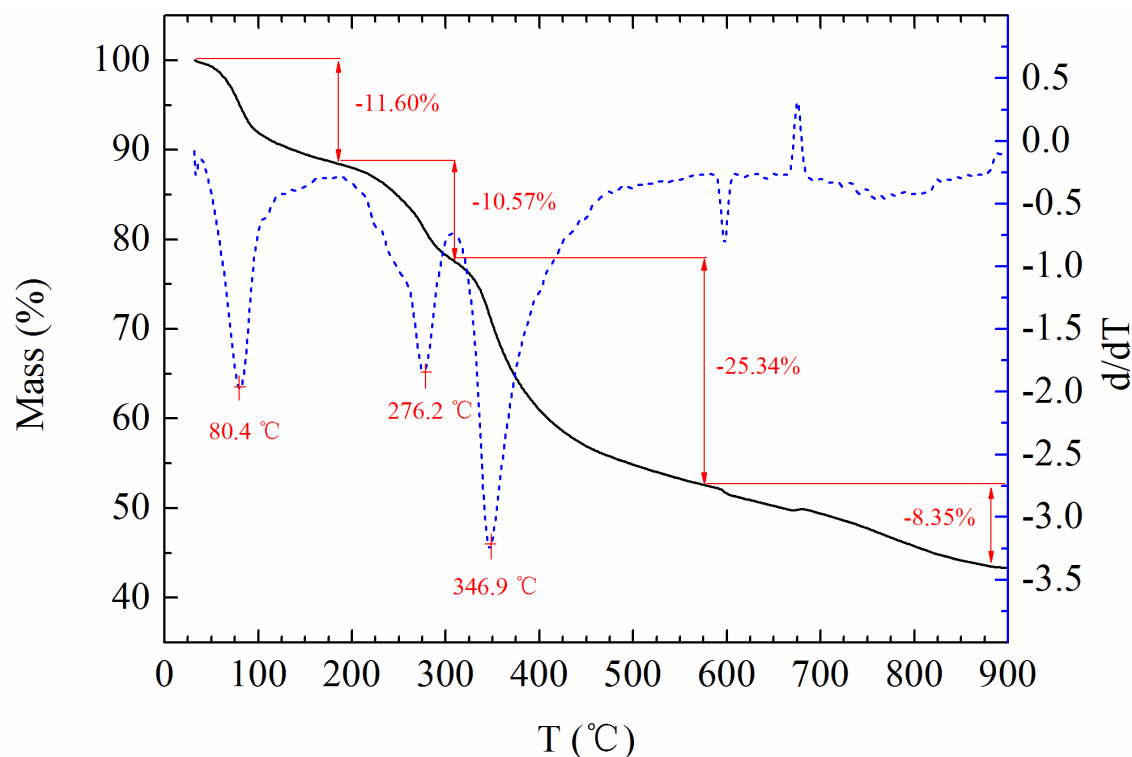


Figure S6. TG curves of solid $K_{3n}[Zn(H_2O)_2]_{1.5n}[Fe_2V_6O_{11}(\text{mal})_6]_n \cdot 6.5nH_2O$ (**4-Zn**).

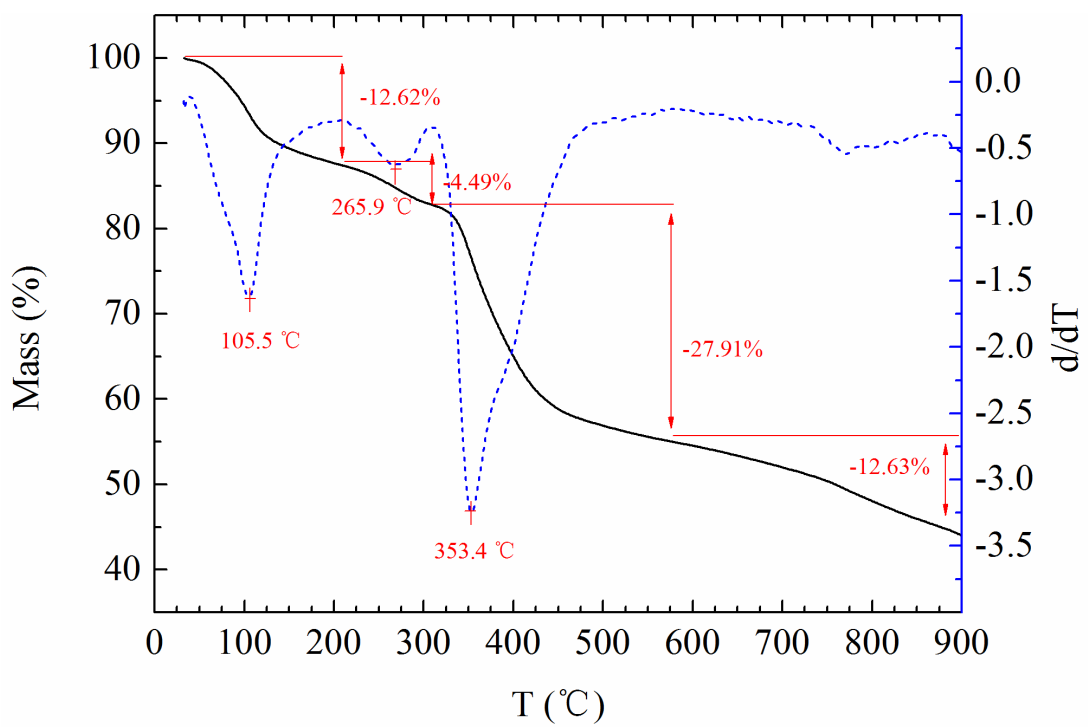


Figure S7. The experimental and simulated PXRD patterns of **2**-Fe.

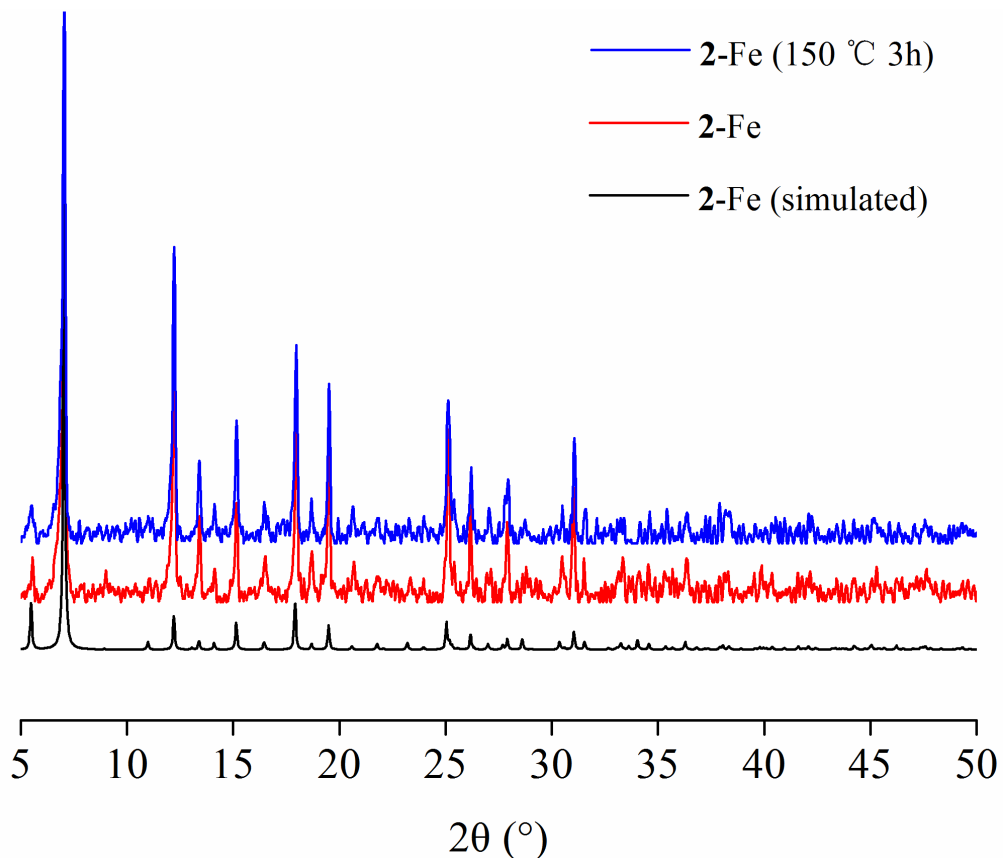


Figure S8. The experimental and simulated PXRD patterns of **3-Cu**.

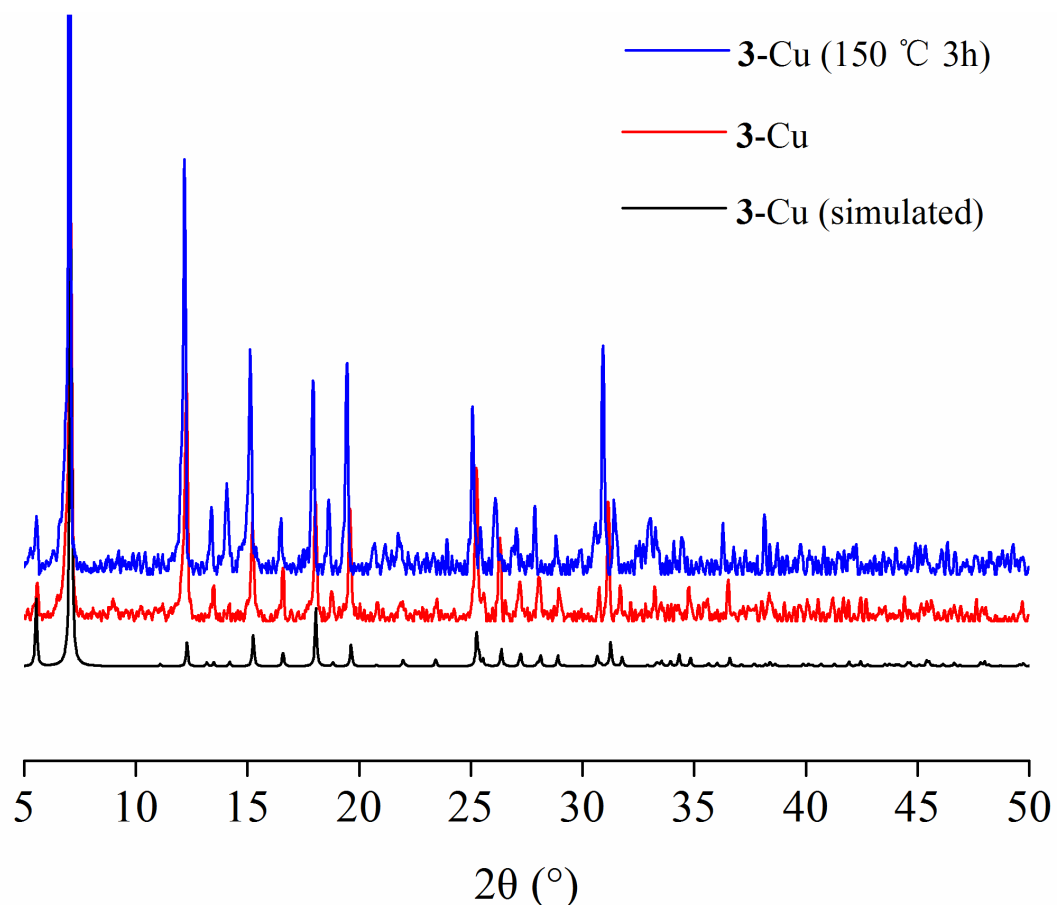


Figure S9. The experimental and simulated PXRD patterns of **4-Zn**.

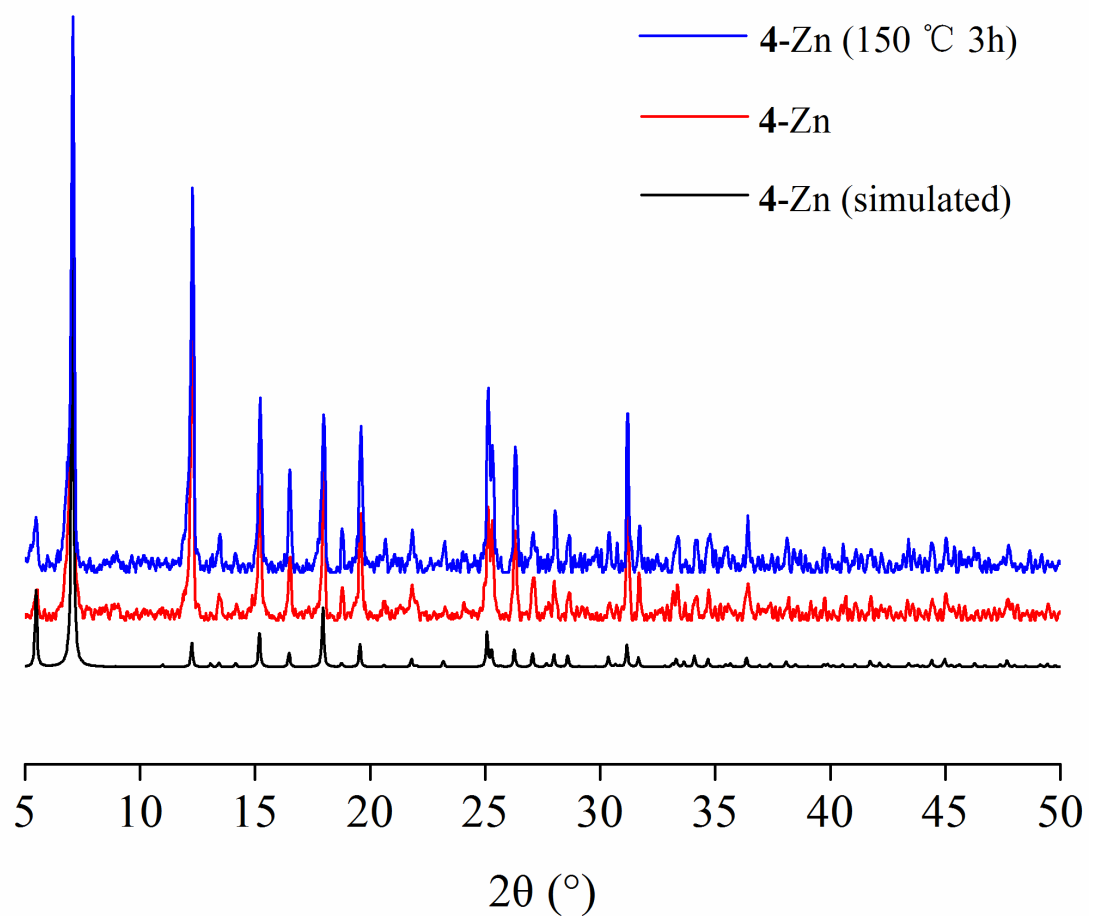


Figure S10. N₂ adsorption-desorption isotherms of **2 ~ 4** at 77K.

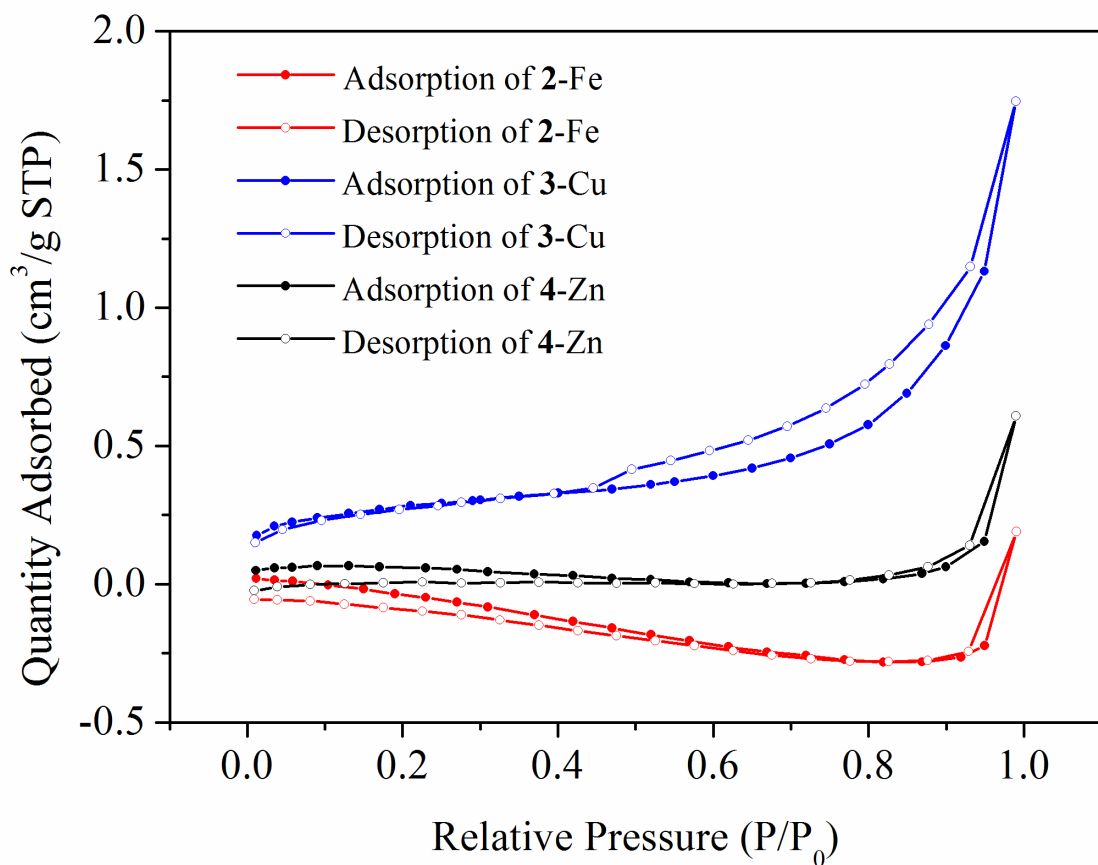


Figure S11. Linear fits of O₂ adsorptions and desorptions at 298 K for **2 ~ 4**.

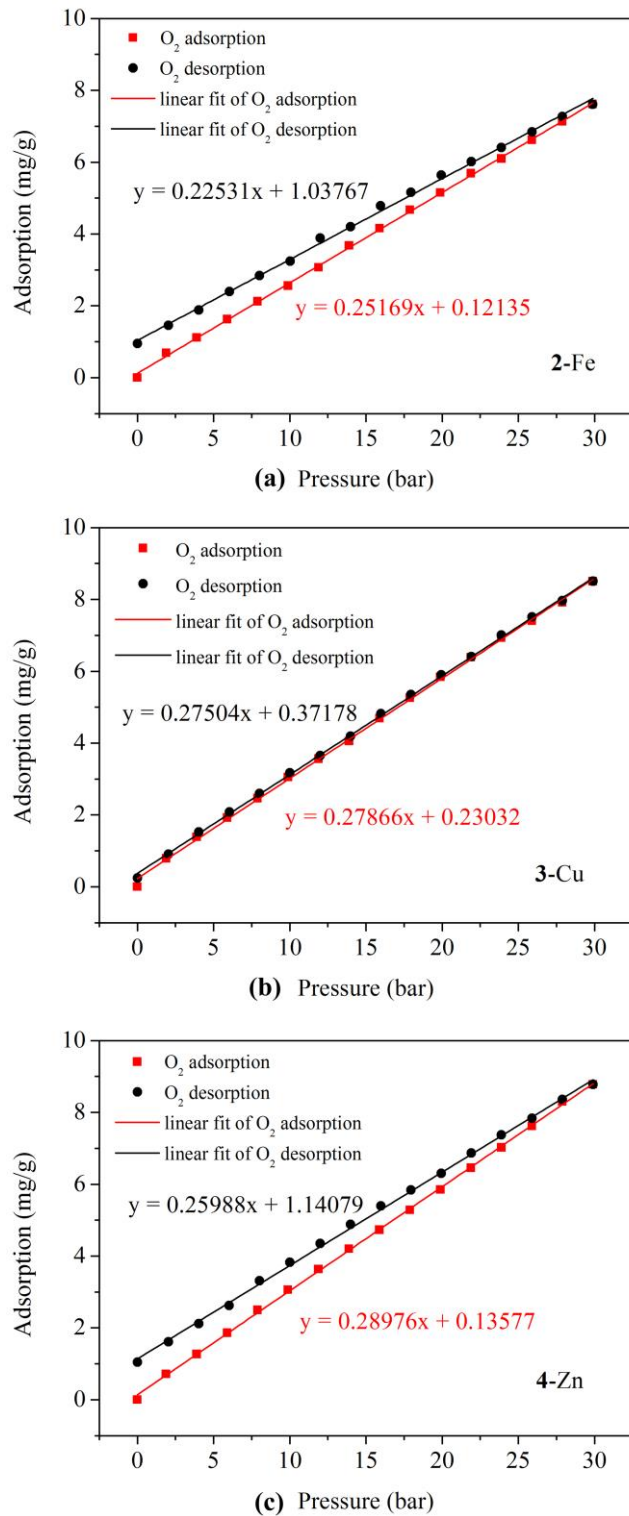


Figure S12. Linear fits of O₂ adsorptions at 308 K for **2 ~ 4**.

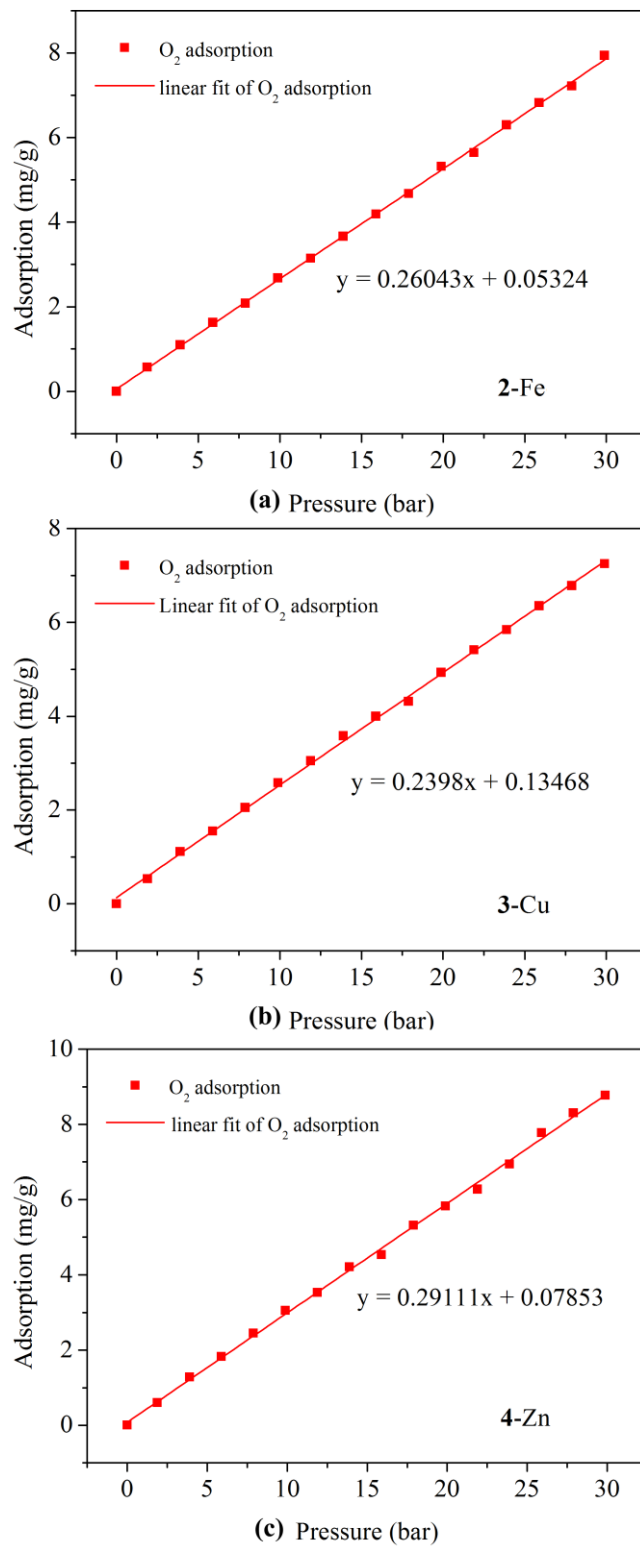
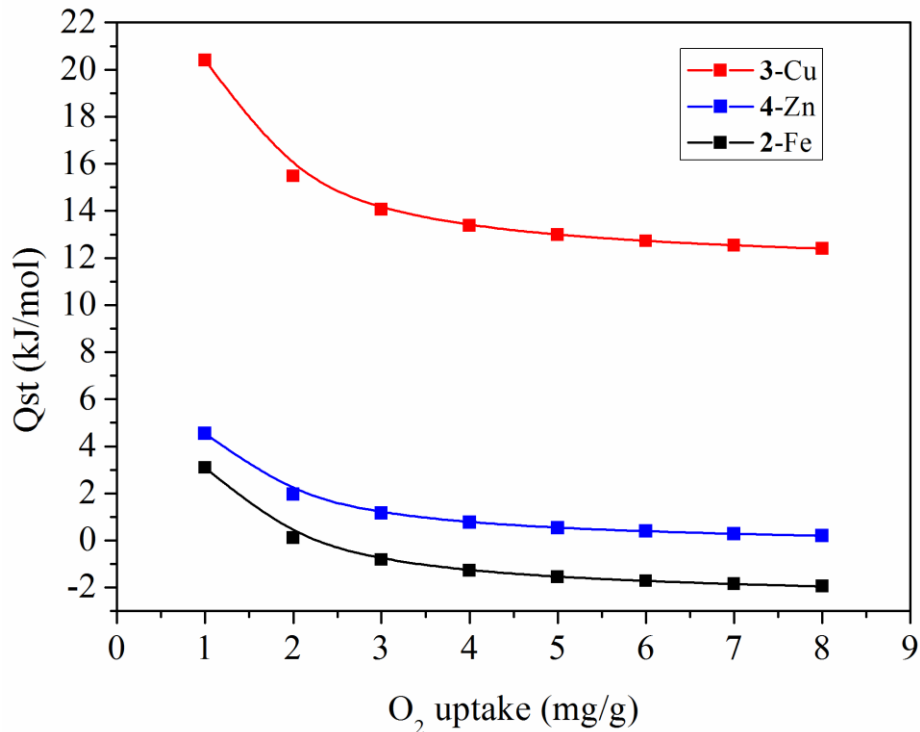


Figure S13. Isosteric heat of adsorption (Q_{st}) plotted against O₂ uptake for **2 ~ 4**.



Isosteric heat of adsorption was calculated using Clausius–Clapeyron equation:

$$Q_{st} = RT_1T_2 \ln(P_2/P_1)/(T_2-T_1)$$

$$R = 8.314 \times 10^{-3} \text{ kJ/(mol}\cdot\text{K}^{-1}), T_1 = 298 \text{ K}, T_2 = 308 \text{ K};$$

Linear fitting equation of the sorption isotherms at 298 and 308 K respectively (Figures S11 and S12):

2-Fe:

$$P_1 = (m - 0.12135)/0.25169$$

$$P_2 = (m - 0.05324)/0.26043$$

3-Cu:

$$P_1 = (m - 0.23032)/0.27866$$

$$P_2 = (m - 0.13468)/0.2398$$

4-Zn:

$$P_1 = (m - 0.13577)/0.28976$$

$$P_2 = (m - 0.07853)/0.29111$$

Figure S14. FT-infrared spectra of $(\text{NH}_4)_3(\text{NH}_3\text{CH}_3)_3[\text{Fe}_2\text{V}_6\text{O}_{11}(\text{mal})_6] \cdot 7.5\text{H}_2\text{O}$ (**1**), $(\text{NH}_4)_{3n}[\text{Fe}(\text{H}_2\text{O})_2]_{1.5n}[\text{Fe}_2\text{V}_6\text{O}_{11}(\text{mal})_6]_n \cdot 7.5n\text{H}_2\text{O}$ (**2-Fe**), $\text{K}_{3n}[\text{Cu}(\text{H}_2\text{O})_2]_{1.5n}[\text{Fe}_2\text{V}_6\text{O}_{11}(\text{mal})_6]_n \cdot 10n\text{H}_2\text{O}$ (**3-Cu**) and $\text{K}_{3n}[\text{Zn}(\text{H}_2\text{O})_2]_{1.5n}[\text{Fe}_2\text{V}_6\text{O}_{11}(\text{mal})_6]_n \cdot 6.5n\text{H}_2\text{O}$ (**4-Zn**).

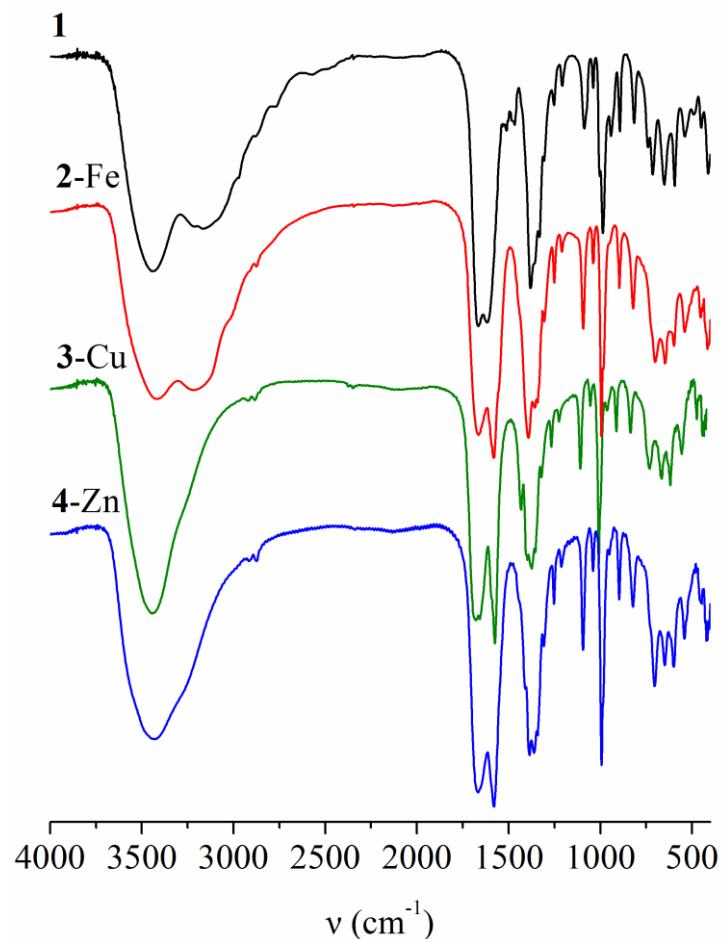


Figure S15. FT-infrared spectra of **2**-Fe, **2**-Fe-O₂. The sample of **2**-Fe-O₂ were treated with O₂ adsorption.

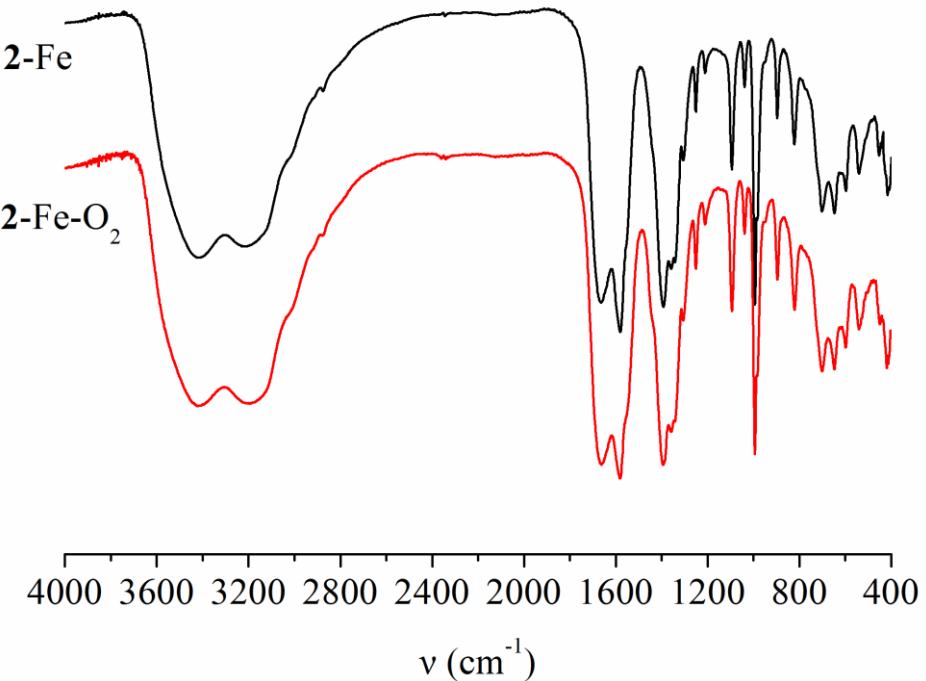


Figure S16. Diffused reflectance spectra of solids (**1**), (**2-Fe**), (**3-Cu**) and (**4-Zn**).

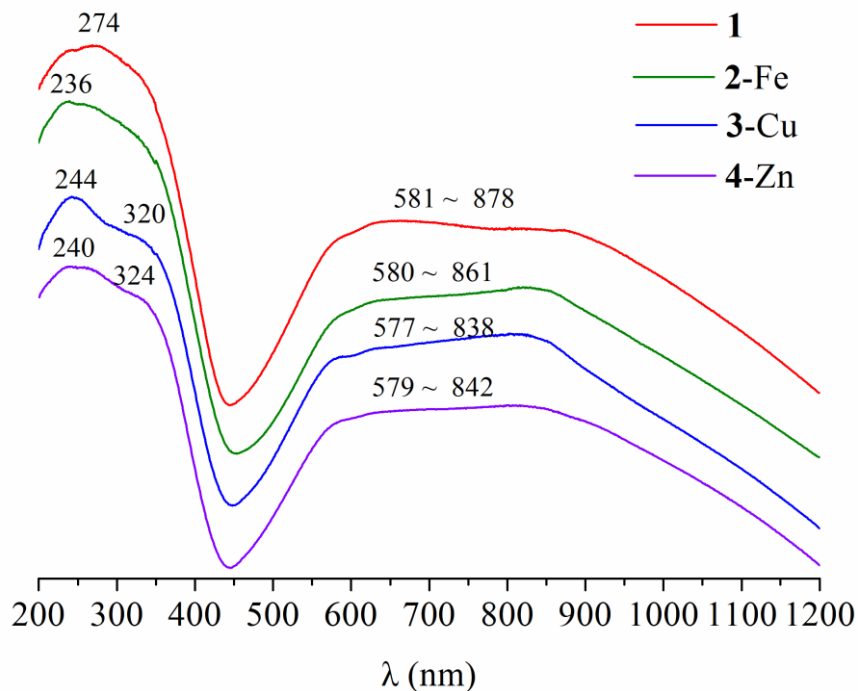


Figure S17. The solid diffused spectra of **2**-Fe and **2**-Fe-O₂. The sample of **2**-Fe-O₂ were treated with O₂ adsorption.

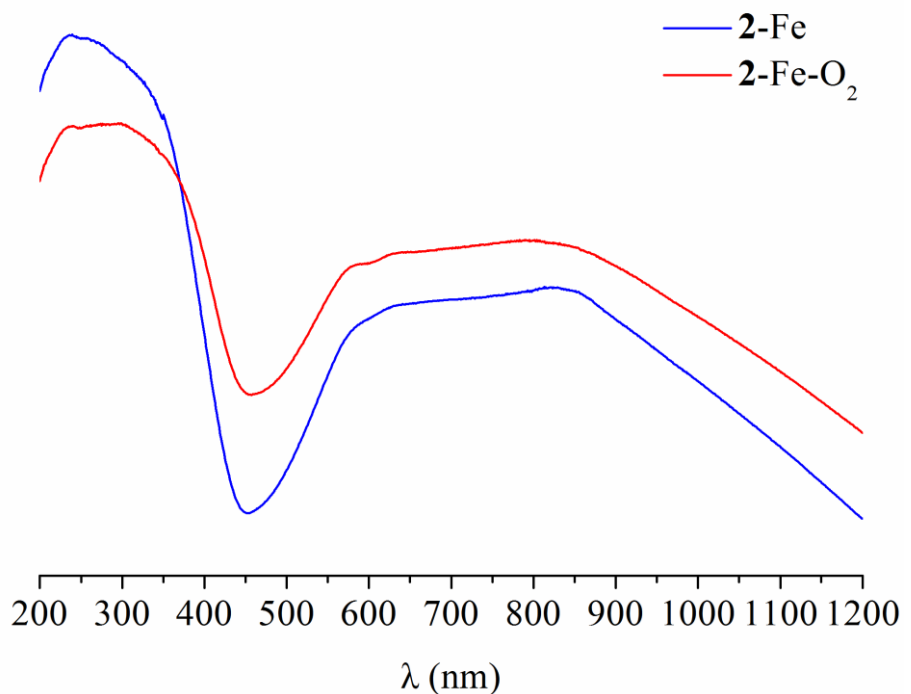


Figure S18. The EPR spectra of **1**, **2-Fe** and **4-Zn** in solid state at 100 K.

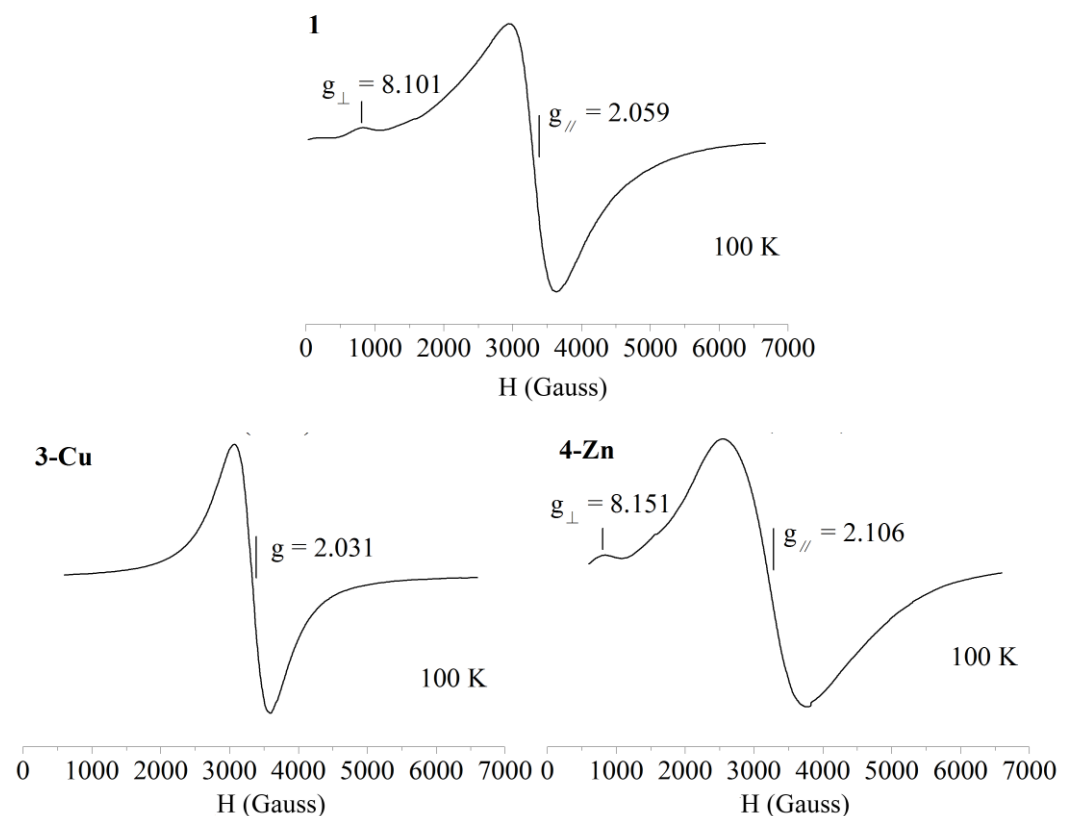


Table S1. Crystallographic data and structural refinement details for $(\text{NH}_4)_3(\text{NH}_3\text{CH}_3)_3[\text{Fe}_2\text{V}_6\text{O}_{11}(\text{mal})_6] \cdot 7.5\text{H}_2\text{O}$ (**1**), $(\text{NH}_4)_{3n}[\text{Fe}(\text{H}_2\text{O})_2]_{1.5n}[\text{Fe}_2\text{V}_6\text{O}_{11}(\text{mal})_6]_n \cdot 7.5n\text{H}_2\text{O}$ (**2-Fe**), $\text{K}_{3n}[\text{Cu}(\text{H}_2\text{O})_2]_{1.5n}[\text{Fe}_2\text{V}_6\text{O}_{11}(\text{mal})_6]_n \cdot 10n\text{H}_2\text{O}$ (**3-Cu**) and $\text{K}_{3n}[\text{Zn}(\text{H}_2\text{O})_2]_{1.5n}[\text{Fe}_2\text{V}_6\text{O}_{11}(\text{mal})_6]_n \cdot 6.5n\text{H}_2\text{O}$ (**4-Zn**).

	1	2-Fe	3-Cu	4-Zn
Empirical formula	$\text{C}_{27}\text{H}_{63}\text{Fe}_2\text{N}_6\text{O}_{48.5}\text{V}_6$	$\text{C}_{24}\text{H}_{51}\text{Fe}_{3.5}\text{N}_3\text{O}_{51.5}\text{V}_6$	$\text{C}_{24}\text{H}_{44}\text{Fe}_2\text{K}_3\text{O}_{54}\text{V}_6\text{Cu}_{1.5}$	$\text{C}_{24}\text{H}_{37}\text{Fe}_2\text{K}_3\text{O}_{50.5}\text{V}_6\text{Zn}_{1.5}$
Formula weight	1665.17	1706.79	1826.54	1766.27
Temperature, K			193	
Wavelength, Å			0.71073	
Crystal system			hexagonal	
Space group	<i>P</i> -6	<i>P</i> 6/ <i>m</i>	<i>P</i> 6/ <i>m</i>	<i>P</i> 6/ <i>m</i>
Unit cell dimensions				
<i>a</i> , Å	15.0917(8)	14.4915(4)	14.3904(6)	14.4380(5)
<i>b</i> , Å	15.0917(8)	14.4915(4)	14.3904(6)	14.4380(5)
<i>c</i> , Å	17.170(1)	16.0927(4)	15.9322(5)	16.1108(5)
α , °			90	
β , °			90	
γ , °			120	
<i>V</i> , Å ³	3386.7(4)	2926.8(2)	2857.3(3)	2908.4(2)
<i>Z</i>			2	
<i>D</i> (calculated), g/cm ³	1.633	1.937	2.123	2.007
Abs. coeff., mm ⁻¹	1.312	1.876	2.321	2.341
<i>F</i> (000)	1690.0	1714.0	1821.0	1744.0
Crystal size, mm	0.30 × 0.20 × 0.10	0.38 × 0.3 × 0.3	0.3 × 0.1 × 0.07	0.3 × 0.1 × 0.1
2θ range for data collection, deg	5.398 ~ 49.998	6.014 ~ 57.906	5.114 ~ 58.062	5.056 ~ 57.692
Reflections collected	6927	8417	11004	10746
Independent reflections	3945	2388	2380	2400
<i>R</i> _{int}	0.0514	0.0292	0.0470	0.0524
Data / restraints / parameters	3945/27/282	2388/12/138	2380/0/129	2400/93/131
GOF on <i>F</i> ²	1.008	1.050	1.063	1.009
Final <i>R</i> indices <i>R</i> 1 [<i>I</i> > 2σ(<i>I</i>)]	0.0581	0.0436	0.0522	0.0558
<i>R</i> 2 [<i>I</i> > 2σ(<i>I</i>)]	0.1378	0.1192	0.1604	0.1651
Largest diff. peak and hole, eÅ ⁻³	0.86/-0.52	0.54/-1.23	1.76/-1.64	1.83/-1.12

Table S2. Selected bond distances (\AA) and angles ($^\circ$) for $(\text{NH}_4)_3(\text{NH}_3\text{CH}_3)_3[\text{Fe}_2\text{V}_6\text{O}_{11}(\text{mal})_6] \cdot 7.5\text{H}_2\text{O}$ (1).

1			
Fe(1)–O(5) ¹	2.017(8)	Fe(2)–O(13)	2.026(9)
Fe(1)–O(5)	2.017(8)	Fe(2)–O(13) ³	2.026(9)
Fe(1)–O(5) ²	2.017(8)	Fe(2)–O(13) ⁴	2.026(9)
Fe(1)–O(6)	2.008(8)	Fe(2)–O(14)	1.99 (1)
Fe(1)–O(6) ¹	2.008(8)	Fe(2)–O(14) ⁴	1.99(1)
Fe(1)–O(6) ²	2.008(8)	Fe(2)–O(14) ³	1.99(1)
V(1)–O(3)	1.907(2)	V(2)–O(13)	2.004(9)
V(1)–O(4)	2.002(9)	V(2)–O(9)	1.58(1)
V(1)–O(5)	1.988(8)	V(2)–O(12)	1.965(9)
V(1)–O(2)	1.834(5)	V(2)–O(10)	1.818(4)
V(1)–O(1)	1.596(9)	V(2)–O(11)	1.914(2)
Symmetric transformations: ¹ 1 + y – x, 2 – x, +z; ² 2 – y, 1 + x – y, +z; ³ 1 – y, 1 + x – y, +z; ⁴ y – x, 1 – x, +z.			
O(5) ¹ –Fe(1)–O(5)	93.1(3)	O(14) ³ –Fe(2)–O(13) ⁴	91.0(4)
O(5) ² –Fe(1)–O(5)	93.1(3)	O(14) ⁴ –Fe(2)–O(13) ⁴	87.3(4)
O(5) ² –Fe(1)–O(5) ¹	93.1(3)	O(14)–Fe(2)–O(13) ³	91.0(4)
O(6)–Fe(1)–O(5)	88.1(3)	O(14) ⁴ –Fe(2)–O(13)	91.0(4)
O(6) ² –Fe(1)–O(5)	91.7(4)	O(14)–Fe(2)–O(13)	87.3(4)
O(6)–Fe(1)–O(5) ²	174.9(4)	O(14) ⁴ –Fe(2)–O(13) ³	174.1(4)
O(6) ² –Fe(1)–O(5) ¹	174.9(4)	O(14) ³ –Fe(2)–O(13) ³	87.3(4)
O(6)–Fe(1)–O(5) ¹	91.7(3)	O(14)–Fe(2)–O(14) ³	87.1(4)
O(6) ¹ –Fe(1)–O(5)	174.9(4)	O(14) ³ –Fe(2)–O(14) ⁴	87.1(4)
O(6) ¹ –Fe(1)–O(5) ¹	88.1(3)	O(14)–Fe(2)–O(14) ⁴	87.1(5)
O(6) ² –Fe(1)–O(5) ²	88.1(3)	O(9)–V(2)–O(13)	107.1(5)
O(6) ¹ –Fe(1)–O(5) ²	91.7(4)	O(9)–V(2)–O(12)	106.3(5)
O(6) ² –Fe(1)–O(6)	86.9(4)	O(9)–V(2)–O(10)	107.4(5)
O(6) ² –Fe(1)–O(6) ¹	86.9(4)	O(9)–V(2)–O(11)	102.8(4)
O(6) ¹ –Fe(1)–O(6)	86.9(4)	O(12)–V(2)–O(13)	78.9(4)
O(3)–V(1)–O(4)	150.7(3)	O(10)–V(2)–O(13)	145.4(5)
O(3)–V(1)–O(5)	84.4(4)	O(10)–V(2)–O(12)	89.1(5)
O(5)–V(1)–O(4)	78.7(3)	O(10)–V(2)–O(11)	92.4(6)
O(2)–V(1)–O(3)	93.3(5)	O(11)–V(2)–O(13)	82.6(5)
O(2)–V(1)–O(4)	88.1(4)	O(11)–V(2)–O(12)	149.0(3)
O(2)–V(1)–O(5)	146.9(4)	V(1) ¹ –O(3)–V(1) ²	119.90(4)
O(1)–V(1)–O(3)	102.2(3)	V(1)–O(3)–V(1) ¹	119.89(4)
O(1)–V(1)–O(4)	105.2(4)	V(1)–O(3)–V(1) ²	119.90(4)
O(1)–V(1)–O(5)	105.3(4)	V(1)–O(5)–Fe(1)	127.0(4)
O(1)–V(1)–O(2)	107.5(5)	V(1)–O(2)–V(1) ⁵	134.3(7)
O(13) ³ –Fe(2)–O(13)	94.4(3)	V(2)–O(13)–Fe(2)	122.9(4)

O(13)–Fe(2)–O(13) ⁴	94.4(3)	V(2) ⁵ –O(10)–V(2)	143.4(7)
O(13) ³ –Fe(2)–O(13) ⁴	94.4(3)	V(2) ³ –O(11)–V(2)	119.97(3)
O(14) ³ –Fe(2)–O(13)	174.1(4)	V(2) ³ –O(11)–V(2) ⁴	119.97(3)
O(14)–Fe(2)–O(13) ⁴	174.1(4)	V(2) ⁴ –O(11)–V(2)	119.97(3)
Symmetric transformations: ¹ 1 + $y - x$, 2 – x , + z ; ² 2 – y , 1 + $x - y$, + z ; ³ 1 – y , 1 + $x - y$, + z ; ⁴ $y - x$, 1 – x , + z ; ⁵ + x , + y , 2 – z .			

Table S3. Selected bond distances (\AA) and angles ($^{\circ}$) for $(\text{NH}_4)_{3n}[\text{Fe}(\text{H}_2\text{O})_2]_{1.5n}[\text{Fe}_2\text{V}_6\text{O}_{11}(\text{mal})_6]_n \cdot 7.5n\text{H}_2\text{O}$ (**2-Fe**).

2-Fe

V(1)–O(4)	2.012(2)	Fe(1)–O(7) ²	2.026(2)
V(1)–O(5)	1.974(2)	Fe(1)–O(7) ¹	2.026(2)
V(1)–O(3)	1.9033(5)	Fe(2)–O(8) ³	2.111(4)
V(1)–O(2)	1.813(1)	Fe(2)–O(8)	2.111(4)
V(1)–O(1)	1.599(2)	Fe(2)–O(8) ⁴	2.111(4)
Fe(1)–O(4) ¹	1.998(2)	Fe(2)–O(8) ⁵	2.111(4)
Fe(1)–O(4) ²	1.998(2)	Fe(2)–O(1w) ⁴	2.146(5)
Fe(1)–O(4)	1.998(2)	Fe(2)–O(1w)	2.146(5)
Fe(1)–O(7)	2.026(2)		
Symmetry transformation: ¹ 1 + $y - x$, 1 - x , + z ; ² 1 - y , + $x - y$, + z ; ³ 1 - x , - y , + z ; ⁴ 1 - x , - y , 1 - z ; ⁵ + x , + y , 1 - z .			
O(5)–V(1)–O(4)	78.84(9)	O(7) ¹ –Fe(1)–O(7) ²	85.8(1)
O(3)–V(1)–O(4)	82.8(1)	O(7)–Fe(1)–O(7) ¹	85.8(1)
O(3)–V(1)–O(5)	147.82(9)	O(8) ³ –Fe(2)–O(8) ⁴	88.4(2)
O(2)–V(1)–O(4)	144.8(1)	O(8) ⁵ –Fe(2)–O(8) ⁴	91.6(2)
O(2)–V(1)–O(5)	87.6(1)	O(8) ³ –Fe(2)–O(8) ⁵	180.0(1)
O(2)–V(1)–O(3)	92.6(1)	O(8) ³ –Fe(2)–O(8)	91.6(2)
O(1)–V(1)–O(4)	108.0(1)	O(8) ⁵ –Fe(2)–O(8)	88.4(2)
O(1)–V(1)–O(5)	108.8(1)	O(8) ⁴ –Fe(2)–O(8)	180
O(1)–V(1)–O(3)	101.84(9)	O(8) ³ –Fe(2)–O(1w) ⁴	92.9(2)
O(1)–V(1)–O(2)	107.1(1)	O(8) ⁴ –Fe(2)–O(1w)	92.9(2)
O(4) ¹ –Fe(1)–O(4) ²	94.11(8)	O(8) ³ –Fe(2)–O(1w)	87.1(2)
O(4) ² –Fe(1)–O(4)	94.11(8)	O(8) ⁴ –Fe(2)–O(1w) ⁴	87.1(2)
O(4) ¹ –Fe(1)–O(4)	94.12(8)	O(8)–Fe(2)–O(1w) ⁴	92.9(2)
O(4) ¹ –Fe(1)–O(7)	91.0(1)	O(8) ⁵ –Fe(2)–O(1w) ⁴	87.1(2)
O(4)–Fe(1)–O(7) ¹	173.9(1)	O(8) ⁵ –Fe(2)–O(1w)	92.9(2)
O(4) ² –Fe(1)–O(7) ¹	91.0(1)	O(8)–Fe(2)–O(1w)	87.1(2)
O(4)–Fe(1)–O(7) ²	91.0(1)	O(1w) ⁴ –Fe(2)–O(1w)	180
O(4)–Fe(1)–O(7)	88.8(1)	Fe(1)–O(4)–V(1)	123.4(1)
O(4) ² –Fe(1)–O(7)	173.9(1)	V(1) ¹ –O(3)–V(1)	119.91(1)
O(4) ² –Fe(1)–O(7) ²	88.8(1)	V(1) ² –O(3)–V(1)	119.91(1)
O(4) ¹ –Fe(1)–O(7) ²	173.9(1)	V(1) ¹ –O(3)–V(1) ²	119.92(1)
O(4) ¹ –Fe(1)–O(7) ¹	88.8(1)	V(1) ⁶ –O(2)–V(1)	141.8(2)
O(7)–Fe(1)–O(7) ²	85.8(1)		
Symmetric transformations: ¹ 1 - y , + $x - y$, + x ; ² 1 + $y - x$, 1 - x , + z ; ³ + x , + y , 1 - z ; ⁴ 1 - x , - y , 1 - z ; ⁵ 1 - x , - y , + z ; ⁶ + x , + y , 2 - z .			

Table S4. Selected bond distances (\AA) and angles ($^{\circ}$) for $\text{K}_{3n}[\text{Cu}(\text{H}_2\text{O})_2]_{1.5n}[\text{Fe}_2\text{V}_6\text{O}_{11}(\text{mal})_6]_n \cdot 10n\text{H}_2\text{O}$ (**3-Cu**).

3-Cu			
Cu(1)–O(8)	1.982(3)	Fe(1)–O(7) ⁴	2.037(3)
Cu(1)–O(8) ¹	1.982(3)	Fe(1)–O(7) ⁵	2.037(3)
Cu(1)–O(8) ²	1.982(3)	Fe(1)–O(7)	2.037(3)
Cu(1)–O(8) ³	1.982(3)	V(1)–O(4)	2.012(3)
Cu(1)–O(1w)	2.379(5)	V(1)–O(3)	1.9052(8)
Cu(1)–O(1w) ²	2.379(5)	V(1)–O(5)	1.963(3)
Fe(1)–O(4) ⁴	1.988(3)	V(1)–O(2)	1.810(2)
Fe(1)–O(4) ⁵	1.988(3)	V(1)–O(1)	1.596(4)
Fe(1)–O(4)	1.988(3)		
Symmetry transformation: ¹ + x , + y , - z ; ² 1 - x , 2 - y , - z ; ³ 1 - x , 2 - y , + z ; ⁴ 1 - y , 1 + x - y , + z ; ⁵ + y - x , 1 - x , + z .			
O(8)–Cu(1)–O(8) ¹	180	O(4) ⁴ –Fe(1)–O(7)	90.3(1)
O(8)–Cu(1)–O(8) ²	91.5(2)	O(4) ⁵ –Fe(1)–O(7) ⁵	88.7(1)
O(8) ¹ –Cu(1)–O(8) ²	88.5(2)	O(4) ⁴ –Fe(1)–O(7) ⁵	173.2(1)
O(8)–Cu(1)–O(8) ³	88.5(2)	O(4)–Fe(1)–O(7) ⁴	173.2(1)
O(8) ¹ –Cu(1)–O(8) ³	91.5(2)	O(7) ⁴ –Fe(1)–O(7) ⁵	85.6(1)
O(8) ² –Cu(1)–O(8) ³	180	O(7)–Fe(1)–O(7) ⁵	85.6(1)
O(8) ¹ –Cu(1)–O(1w) ¹	85.2(1)	O(7) ⁴ –Fe(1)–O(7)	85.6(1)
O(8)–Cu(1)–O(1w) ¹	94.8(1)	O(3)–V(1)–O(4)	82.7(2)
O(8) ³ –Cu(1)–O(1w) ¹	85.2(1)	O(3)–V(1)–O(5)	148.6(1)
O(8) ¹ –Cu(1)–O(1w)	94.8(1)	O(5)–V(1)–O(4)	79.0(1)
O(8) ² –Cu(1)–O(1w) ¹	94.8(1)	O(2)–V(1)–O(4)	145.2(2)
O(8) ² –Cu(1)–O(1w)	85.2(1)	O(2)–V(1)–O(3)	92.9(2)
O(8) ³ –Cu(1)–O(1w)	94.8(1)	O(2)–V(1)–O(5)	88.0(2)
O(8)–Cu(1)–O(1w)	85.2(1)	O(1)–V(1)–O(4)	107.9(2)
O(1w)–Cu(1)–O(1w) ¹	180	O(1)–V(1)–O(3)	101.6(1)
O(4) ⁴ –Fe(1)–O(4)	95.0(1)	O(1)–V(1)–O(5)	108.2(2)
O(4) ⁴ –Fe(1)–O(4) ⁵	95.0(1)	O(1)–V(1)–O(2)	106.8(2)
O(4) ⁵ –Fe(1)–O(4)	95.0(1)	Fe(1)–O(4)–V(1)	122.7(1)
O(4)–Fe(1)–O(7)	88.7(1)	V(1) ⁴ –O(3)–V(1)	119.92(1)
O(4) ⁵ –Fe(1)–O(7)	173.2(1)	V(1) ⁴ –O(3)–V(1) ⁵	119.92(1)
O(4) ⁵ –Fe(1)–O(7) ⁴	90.3(1)	V(1) ⁵ –O(3)–V(1)	119.92(2)
O(4) ⁴ –Fe(1)–O(7) ⁴	88.7(1)	V(1) ¹⁰ –O(2)–V(1)	142.5(3)
O(4)–Fe(1)–O(7) ⁵	90.3(1)		
Symmetric transformations: ¹ 1 - x , 2 - y , - z ; ² + x , + y , - z ; ³ 1 - x , 2 - y , + z ; ⁴ 1 - y , 1 + x - y , + z ; ⁵ + y - x , 1 - x , + z ; ⁶ 1 - x , 1 - y , 1 - z ; ⁷ 1 - x , 1 - y , + z ; ⁸ + y , - x + y , 1 - z ; ⁹ - y + x , + x , 1 - z ; ¹⁰ + x , + y , 1 - z .			

Table S5. Selected bond distances (\AA) and angles ($^{\circ}$) for $\text{K}_{3n}[\text{Zn}(\text{H}_2\text{O})_2]_{1.5n}[\text{Fe}_2\text{V}_6\text{O}_{11}(\text{mal})_6]_n \cdot 6.5n\text{H}_2\text{O}$ (**4-Zn**).

4-Zn

Zn(1)–O(1w) ¹	2.122(5)	Fe(1)–O(7) ⁵	2.033(3)
Zn(1)–O(1w)	2.122(5)	Fe(1)–O(7) ⁴	2.033(3)
Zn(1)–O(8) ²	2.082(4)	Fe(1)–O(7)	2.033(3)
Zn(1)–O(8) ³	2.082(4)	V(1)–O(3)	1.9051(8)
Zn(1)–O(8) ¹	2.082(4)	V(1)–O(4)	2.012(3)
Zn(1)–O(8)	2.082(4)	V(1)–O(2)	1.812(2)
Fe(1)–O(4)	2.001(3)	V(1)–O(5)	1.971(4)
Fe(1)–O(4) ⁴	2.001(3)	V(1)–O(1)	1.592(4)
Fe(1)–O(4) ⁵	2.001(3)		
Symmetry transformation: ¹ - x , -1 - y , 1 - z ; ² - x , -1 - y , + z ; ³ + x , + y , 1 - z ; ⁴ - y , -1 + x - y , + z ; ⁵ 1 + y - x , - x , + z .			
O(1w)–Zn(1)–O(1w) ¹	180	O(4)–Fe(1)–O(7) ⁵	173.7(1)
O(8) ² –Zn(1)–O(1w) ¹	92.6(2)	O(4) ⁵ –Fe(1)–O(7) ⁵	88.9(1)
O(8) ³ –Zn(1)–O(1w)	92.6(2)	O(4) ⁵ –Fe(1)–O(7)	90.8(1)
O(8) ¹ –Zn(1)–O(1w) ¹	87.4(2)	O(4)–Fe(1)–O(7) ⁴	90.8(1)
O(8)–Zn(1)–O(1w) ¹	92.6(2)	O(7)–Fe(1)–O(7) ⁴	85.6(1)
O(8) ¹ –Zn(1)–O(1w)	92.6(2)	O(7)–Fe(1)–O(7) ⁵	85.6(1)
O(8)–Zn(1)–O(1w)	87.4(2)	O(7) ⁴ –Fe(1)–O(7) ⁵	85.6(1)
O(8) ² –Zn(1)–O(1w)	87.4(2)	O(3)–V(1)–O(4)	82.9(2)
O(8) ³ –Zn(1)–O(1w) ¹	87.4(2)	O(3)–V(1)–O(5)	148.0(1)
O(8) ¹ –Zn(1)–O(8)	180.0(2)	O(2)–V(1)–O(3)	92.7(2)
O(8) ¹ –Zn(1)–O(8) ²	88.0(3)	O(2)–V(1)–O(4)	145.4(2)
O(8) ³ –Zn(1)–O(8)	88.0(3)	O(2)–V(1)–O(5)	87.8(2)
O(8) ¹ –Zn(1)–O(8) ³	92.0(3)	O(5)–V(1)–O(4)	78.9(1)
O(8) ² –Zn(1)–O(8) ³	180	O(1)–V(1)–O(3)	101.9(2)
O(8) ² –Zn(1)–O(8)	92.0(3)	O(1)–V(1)–O(4)	107.9(2)
O(4)–Fe(1)–O(4) ⁴	94.3(1)	O(1)–V(1)–O(2)	106.5(2)
O(4) ⁵ –Fe(1)–O(4) ⁴	94.3(1)	O(1)–V(1)–O(5)	108.6(2)
O(4)–Fe(1)–O(4) ⁵	94.3(1)	V(1)–O(3)–V(1) ⁴	119.92(2)
O(4)–Fe(1)–O(7)	88.9(1)	V(1)–O(3)–V(1) ⁵	119.92(2)
O(4) ⁴ –Fe(1)–O(7) ⁴	88.9(1)	V(1) ⁵ –O(3)–V(1) ⁴	119.92(2)
O(4) ⁴ –Fe(1)–O(7) ⁵	90.8(1)	Fe(1)–O(4)–V(1)	123.3(2)
O(4) ⁵ –Fe(1)–O(7) ⁴	173.7(1)	V(1)–O(2)–V(1) ¹⁰	142.5(3)
O(4) ⁴ –Fe(1)–O(7)	173.7(1)		
Symmetric transformations: ¹ - x , -1 - y , 1 - z ; ² + x , + y , 1 - z ; ³ - x , -1 - y , + z ; ⁴ 1 + y - x , - x , + z ; ⁵ - y , -1 + x - y , + x , + z ; ⁶ - y + x , + x , 2 - z ; ⁷ + y , - x + y , + z ; ⁸ + y , - x + y , 2 - z ; ⁹ - y , -1 + x - y , 2 - z ; ¹⁰ + x , + y , 2 - z .			

Table S6. Comparisons of selected bond distances (\AA) in **1** ~ **4**.

Bonds	1	2 -Fe	3 -Cu	4 -Zn	Averages
V=O	1.586 _{av}	1.598(3)	1.596(5)	1.593(4)	1.593(5)
V- μ_2 -O	1.826 _{av}	1.812(2)	1.811(3)	1.812(2)	1.815(3)
V- μ_3 -O	1.911 _{av}	1.904(1)	1.906(1)	1.905(1)	1.907(1)
V-O _{α-alkoxy}	1.996 _{av}	2.011(3)	2.015(4)	2.012(3)	2.009(4)
V-O _{α-carboxy}	1.984 _{av}	1.972(3)	1.970(5)	1.971(4)	1.974(5)
Fe ³⁺ -O _{α-alkoxy}	2.022 _{av}	1.998(3)	1.986(4)	2.001(3)	2.002(4)
Fe ³⁺ -O _{β-carboxy}	1.998 _{av}	2.029(3)	2.037(4)	2.033(3)	2.024(4)
M ²⁺ -O _{β-carboxy}		2.111(4)	1.982(3)	2.083(4)	
M ²⁺ -O _{water}		2.146(5)	2.379(5)	2.123(5)	

Note: M = bridging metals Fe, Cu and Zn

Table S7. Select bond distances (Å) and angles (°) of FeV-co² and **2**-Fe.

M–S/O	Distances(Å)	M–S/O–M	Angle(°)	S/O–M–S/O	Angle(°)
FeV-co²					
V1–S1B	2.326	V1–S1B–Fe5	71.8	S4B–V1–S3B	102
V1–S3B	2.355	V1–S1B–Fe6	74.5	S4B–V1–S1B	104.4
V1–S4B	2.324	V1–S3B–Fe6	74.2	S1B–V1–S3B	98.3
Fe5–S1B	2.270	V1–S3B–Fe7	72.8	S4B–Fe7–S3B	107.8
Fe5–S4B	2.240	V1–S4B–Fe5	72.4	S3B–Fe6–S1B	106.4
Fe6–S1B	2.216	V1–S4B–Fe7	73.7	S4B–Fe5–S1B	109.1
Fe6–S2B	2.213	Fe5–S1B–Fe6	70.9	S5A–Fe7–S4B	119.7
Fe6–S3B	2.206	Fe5–S4B–Fe7	72.3	S5A–Fe7–S3B	117.6
Fe7–S3B	2.258	Fe6–S3B–Fe7	70.2	S2B–Fe6–S1B	121.5
Fe7–S4B	2.241	Fe3–S5A–Fe7	70.8	S2B–Fe6–S3B	115.4
Fe7–S5A	2.254	Fe2–S2B–Fe6	72.8	S1A–Fe4–S4A	110.8
Fe3–S5A	2.231	Fe3–S2A–Fe2	70.9	S4A–Fe3–S2A	105.3
Fe3–S4A	2.261	Fe4–S4A–Fe3	70	S2A–Fe2–S1A	103.6
Fe3–S2A	2.287	Fe4–S1A–Fe2	71.2	S4A–Fe1–S2A	105.2
Fe2–S2B	2.227	Fe1–S1A–Fe2	72.8	S2A–Fe1–S1A	102.2
Fe2–S2A	2.278	Fe1–S1A–Fe4	67.8	S1A–Fe1–S4A	111.7
Fe2–S1A	2.216	Fe1–S2A–Fe2	73.1		
Fe4–S4A	2.348	Fe1–S2A–Fe3	71.7		
Fe4–S1A	2.301	Fe1–S4A–Fe4	66.8		
Fe1–S1A	2.306	Fe1–S4A–Fe3	70.6		
Fe1–S2A	2.231				
Fe1–S4A	2.318				
Averages	2.269		71.6		108.8
2 -Fe					
V(1)–O(2)	1.812(2)	V(1)–O(2)–V(1) ⁶	141.9(3)	O(5)–Fe(1)–O(5) ¹	94.1(1)
V(1)–O(5)	2.011(3)	Fe(1)–O(5)–V(1)	123.5(1)	O(5)–V(1)–O(3)	82.7(2)
Fe(1)–O(5)	1.998(3)	V(1)–O(3)–V(1) ¹	119.92(2)	O(5)–V(1)–O(2)	144.9(2)
V(1)–O(3)	1.904(1)				
Averages	1.931(3)		128.4(3)		107.2(2)

Symmetric transformations: ¹ 1 + y – x, 1 – x, +z; ⁶ +x, +y, 2 – z.

Table S8. Bond valence calculations for end-capped iron and bridging metals in **1** ~ **4**.

Complexes	End-capped Fe			Bridging metal		
	atoms	S_{ij}	$\square \Delta$	atoms	S_{ij}	$\square \Delta$
$(\text{NH}_4)_3(\text{NH}_3\text{CH}_3)_3[\text{Fe}_2\text{V}_6\text{O}_{11}(\text{mal})_6] \cdot 7.5\text{H}_2\text{O}$ (1)	Fe(1)	3.020	+0.020			
	Fe(2)	3.073	+0.073			
$(\text{NH}_4)_{3n}[\text{Fe}(\text{H}_2\text{O})_2]_{1.5n}[\text{Fe}_2\text{V}_6\text{O}_{11}(\text{mal})_6]_n \cdot 7.5n\text{H}_2\text{O}$ (2-Fe)	Fe(1)	3.031	+0.031	Fe(2)	2.124	+0.124
$\text{K}_{3n}[\text{Cu}(\text{H}_2\text{O})_2]_{1.5n}[\text{Fe}_2\text{V}_6\text{O}_{11}(\text{mal})_6]_n \cdot 10n\text{H}_2\text{O}$ (3-Cu)	Fe(1)	3.031	+0.031	Cu(1)	2.065	+0.065
$\text{K}_{3n}[\text{Zn}(\text{H}_2\text{O})_2]_{1.5n}[\text{Fe}_2\text{V}_6\text{O}_{11}(\text{mal})_6]_n \cdot 6.5n\text{H}_2\text{O}$ (4-Zn)	Fe(1)	3.045	+0.045	Zn(1)	2.086	+0.086

Calculation formula: $S_{ij} = \sum \exp[(R_0 - r_{ij})/B]$ (r_{ij} is the bond distance between the cation i and the anion j, and R_0 and B are fitted constants.)

Table S9. Bond valence calculations for vanadium centers in **1 ~ 4**.

Complexes	Atoms	S_{ij} (+4) ^[a]	$\square \Delta$	S_{ij} (+5) ^[b]	$\square \Delta$
$(\text{NH}_4)_3(\text{NH}_3\text{CH}_3)_3[\text{Fe}_2\text{V}_6\text{O}_{11}(\text{mal})_6] \cdot 7.5\text{H}_2\text{O}$ (1)	V(1)	4.388	+0.388	4.620	-0.380
	V(2)	4.535	+0.535	4.774	-0.226
$(\text{NH}_4)_{3n}[\text{Fe}(\text{H}_2\text{O})_2]_{1.5n}[\text{Fe}_2\text{V}_6\text{O}_{11}(\text{mal})_6]_n \cdot 7.5n\text{H}_2\text{O}$ (2-Fe)	V(1)	4.437	+0.437	4.670	-0.330
$\text{K}_{3n}[\text{Cu}(\text{H}_2\text{O})_2]_{1.5n}[\text{Fe}_2\text{V}_6\text{O}_{11}(\text{mal})_6]_n \cdot 10n\text{H}_2\text{O}$ (3-Cu)	V(1)	4.449	+0.449	4.684	-0.316
$\text{K}_{3n}[\text{Zn}(\text{H}_2\text{O})_2]_{1.5n}[\text{Fe}_2\text{V}_6\text{O}_{11}(\text{mal})_6]_n \cdot 6.5n\text{H}_2\text{O}$ (4-Zn)	V(1)	4.435	+0.435	4.669	-0.331
Averages	V	4.447	+0.447	4.681	-0.319

[a] R_0 (+4) = 1.7840 B = 0.37. [b] R_0 (+5) = 1.8030 B = 0.37

Calculation formula: $S_{ij} = \sum \exp[-(R_0 - r_{ij})/B]$ (r_{ij} is the bond distance between the cation i and the anion j, and R_0 and B are fitted constants.)

Table S10. Adsorption data of O₂, CO₂, CH₄, N₂ and H₂ (mg/g) of **3-Cu** at 298 K under different pressures respectively.

Pressures (bar)	O ₂	N ₂	H ₂	CO ₂	CH ₄
0.00	0.00	0.00	0.00	0.00	0.00
1.90	0.74	0.11	0.01	0.35	0.05
3.89	1.42	0.05	0.03	0.51	0.00
5.90	1.92	-0.06	0.00	0.52	0.01
7.90	2.43	-0.09	-0.01	0.45	-0.08
9.90	3.04	-0.11	0.00	0.54	-0.07
11.90	3.57	-0.21	-0.02	0.63	-0.10
13.90	4.09	-0.19	0.01	0.51	-0.21
15.89	4.75	-0.20	-0.07	0.51	-0.33
17.90	5.27	-0.36	-0.03	0.35	-0.37
19.90	5.84	-0.54	-0.02	0.35	-0.39
21.90	6.35	-0.56	-0.03	0.25	-0.40
23.89	6.85	-0.60	0.00	0.15	-0.41
25.90	7.39	-0.66	-0.02	0.04	-0.56
27.89	7.84	-0.65	0.03	-0.13	-0.52
29.90	8.43	-0.84	0.02	-0.17	-0.58

Table S11. Adsorption and desorption data of O₂ (mg/g) of **2-Fe**, **3-Cu**, **4-Zn** at 298 K under different pressures respectively.

Pressures (bar)	2-Fe	3-Cu	4-Zn
0.00	0.00	0.00	0.00
1.90	0.68	0.79	0.71
3.90	1.11	1.39	1.27
5.90	1.62	1.92	1.86
7.89	2.12	2.46	2.49
9.90	2.56	3.05	3.06
11.90	3.07	3.56	3.63
13.90	3.68	4.05	4.20
15.90	4.16	4.69	4.73
17.89	4.67	5.25	5.28
19.90	5.15	5.84	5.85
21.90	5.69	6.39	6.45
23.89	6.09	6.93	7.02
25.90	6.61	7.40	7.62
27.89	7.13	7.91	8.30
29.90	7.61	8.50	8.77
29.90	7.61	8.50	8.77
27.89	7.27	7.96	8.35
25.90	6.84	7.51	7.84
23.90	6.41	7.01	7.37
21.92	6.01	6.41	6.87
19.94	5.64	5.90	6.30
17.96	5.16	5.35	5.84
15.98	4.78	4.82	5.40
13.99	4.20	4.19	4.88
12.01	3.89	3.65	4.35
10.02	3.24	3.17	3.83
8.03	2.84	2.60	3.31
6.04	2.40	2.08	2.62
4.04	1.88	1.52	2.11
2.04	1.46	0.90	1.61
0.01	0.95	0.25	1.05

Table S12. Adsorption data of O₂ (mg/g) of **2-Fe**, **3-Cu**, **4-Zn** at 308 K under different pressures respectively.

Pressures (bar)	2-Fe	3-Cu	4-Zn
0.00	0.00	0.00	0.00
1.89	0.57	0.53	0.60
3.90	1.10	1.11	1.28
5.90	1.63	1.55	1.82
7.90	2.08	2.05	2.45
9.89	2.68	2.58	3.05
11.90	3.14	3.05	3.53
13.89	3.66	3.58	4.21
15.90	4.19	4.00	4.53
17.90	4.67	4.31	5.32
19.90	5.32	4.93	5.83
21.90	5.64	5.41	6.27
23.90	6.30	5.84	6.94
25.90	6.82	6.35	7.77
27.89	7.22	6.78	8.30
29.89	7.94	7.25	8.77

References

- (1) Wang, L.; Fan, H.; Du, C.; Xing, X.; Zhao, Y.; Chen, B.; Wang, L. Synthesis, structure and properties of a Co-crystallized complex based on polyoxovanadate $[V^{IV}_{12}V^V_6O_{42}]^{6-}$ and a mononuclear vanadium complex $[VON(CH_2CH_2O)_3]$. *Inorg. Chem. Commun.* **2016**, *63*, 39–41.
- (2) Sippel, D.; Einsle, O. The structure of vanadium nitrogenase reveals an unusual bridging ligand. *Nat. Chem. Biol.* **2017**, *13*, 956–960.